EUROPEAN ORGANIZATION FOR NUCLEAR RESEARCH

CERN–EP/98–19
2 February 1998

Measurement of the beauty production cross-section in 350 GeV/c π^-–Cu interactions

The BEATRICE Collaboration

M. Adamovich[6], M. Adinolfi[3], Y. Alexandrov[6], C. Angelini[7], F. Antinori[2], C. Bacci[10], D. Barberis[3], D. Barney[5], J. Batten[5], W. Beusch[2], C. Bruschini[3], R. Cardarelli[9], A. Cardini[7], V. Casanova[3], F. Ceradini[10], C. Cianfarani[1], G. Ciapetti[8], M. Dameri[3], G. Darbo[3], A. De Santo[7], A. Di Ciaccio[9], A. Duane[5], J. P. Dufey[2], P. Farthouat[2], V. Flaminio[7], A. Forino[1], B. R. French[2], A. Frenkel[8], C. Gemme[3], R. Gessaroli[1], K. Harrison[7], N. Hummadi[5], R. Hurst[3], A. Kirk[2], F. Lacava[8], J. C. Lassalle[2,†], C. Lazzeroni[7], L. Malferrari[1], S. Maljukov[4], G. Martellotti[8], P. Martinengo[3], P. Mazzanti[1], J. G. McEwen[11], I. Minashvili[4], P. Musico[3], P. Nechaeva[6], A. Nisati[8], D. Orestano[10], B. Osculati[3], M. Palutan[8], M. Passaseo[2], G. Penso[8], E. Petrolo[8], L. Pontecorvo[8], A. Quareni[1], H. Rotscheidt[2], V. Ryzhov[2], C. Roda[7], L. Rossi[3], N. Russakovich[4], C. Salvo[3], R. Santonico[9], G. Schuler[2], A. Semenov[4], A. Solovjev[4], M. Torelli[8], S. Veneziano[8], M. Verzocchi[8], D. Websdale[5], M. Weymann[2], L. Zanello[8] and M. Zavertyaev[6].

Abstract

Using a sample of 10^8 triggered events, produced in π^-–Cu interactions at 350 GeV/c, we have identified 26 beauty events. The estimated background in this sample is 0.6 ± 0.6 events. From these data, assuming a linear A-dependence, we measure a beauty production cross-section integrated over all x_F of $5.7^{+1.3}_{-1.1}$ (stat.)$^{+0.6}_{-0.5}$ (syst.) nb/N.

(Submitted to Nuclear Physics B)

[1] Università di Bologna and INFN, Bologna, Italy.
[2] CERN, Geneva, Switzerland.
[3] Università di Genova and INFN, Genoa, Italy.
[4] JINR, Dubna, Russian Federation.
[5] Blackett Laboratory, Imperial College, London, United Kingdom.
[6] Lebedev Physical Institute, Moscow, Russian Federation.
[7] Università di Pisa and INFN, Pisa, Italy.
[8] Università di Roma "La Sapienza" and INFN, Rome, Italy.
[9] Università di Roma "Tor Vergata" and INFN, Rome, Italy.
[10] Università di Roma "Roma Tre" and INFN, Rome, Italy.
[11] University of Southampton, Southampton, United Kingdom.
[†] Deceased

1 Introduction

Descriptions of heavy quark hadroproduction have been developed in the context of perturbative QCD, with complete calculations performed to next-to-leading-order [1]. The theoretical predictions are affected by uncertainties relating to the choice of parton-distribution functions, quark masses, factorization scale and renormalization scale. The next-to-leading-order predictions for the production of $b\bar{b}$ pairs in hadron–nucleon interactions at fixed-target energies have an uncertainty of about an order of magnitude. Experimental measurements, though few in number, have reached a better precision, and so constrain the choice of parameters. The beauty production cross-section in π^-–nucleon collisions at $\sqrt{s} \approx 25$–30 GeV is of the order of a few nanobarns per nucleon, representing a fraction $\sim 10^{-7}$ of the inelastic cross-section. To cope with the unfavorable signal-to-background ratio, two different approaches have been used in previous experiments:

– high luminosity beam-dump experiments have selected semi-leptonic decays through muon detection and a consideration of any missing energy in the final state. This technique provided the very first measurement of beauty hadroproduction, obtained in the WA78 [2] experiment: using a 320 GeV/c π^- beam on U, and assuming a mixing parameter $\chi_d = 0.16$ [3], a cross-section of $3.2 \pm 0.4 \pm 1.0$ nb/N was measured;

– high-resolution tracking detectors have been used to identify multiple decay vertices. To date, the richest sample of events so selected consists of 9 events, identified in the E653 experiment [4]. This experiment, with a trigger requiring at least one muon and an interaction in the emulsion target, measured an inclusive $b\bar{b}$ cross-section of $33 \pm 11 \pm 6$ nb/N in 600 GeV/c π^- interactions.

The WA92 experiment, performed by the BEATRICE collaboration at the CERN Super Proton Synchrotron, chose to exploit both the high luminosity provided by an intense π^- beam on a heavy target and the imaging capabilities of a high-resolution tracking detector that measured secondary vertices immediately downstream of the target. This detector was complemented by a spectrometer and a trigger that exploited the main characteristics of the decays of beauty particles: their lifetimes, which result in impact parameters of the order of a few hundred microns and decay paths of several millimeters; their large probability for producing leptons in the final state; their high mass, which favours decay products with high transverse momentum.

In this paper, we report the WA92 results on the cross-section of beauty particles produced in 350 GeV/c π^-–Cu interactions. The data were taken during 1992 (Cu92 data) and 1993 (Cu93 data) [1)].

2 The WA92 Experiment

2.1 Experimental apparatus and trigger

The experimental apparatus and trigger are described in detail elsewhere [5], and only their main features are outlined here. The apparatus (Fig. 1) consisted of the Ω spectrometer [6], supplemented by a silicon microstrip detector (SMD), installed just upstream of the Ω dipole magnet. The SMD comprised a 2 mm thick Cu target, preceded by a Beam Hodoscope (BmH), and followed by an "in-target" counter (IT), a Decay Detector (DkD), and a Vertex Detector (VxD). The BmH consisted of 10 silicon microstrip planes of 20 μm pitch. The DkD was composed of 17 planes of 10 μm pitch silicon microstrips,

[1)] Some data, not used in the present analysis, were recorded with a tungsten target in 1992.

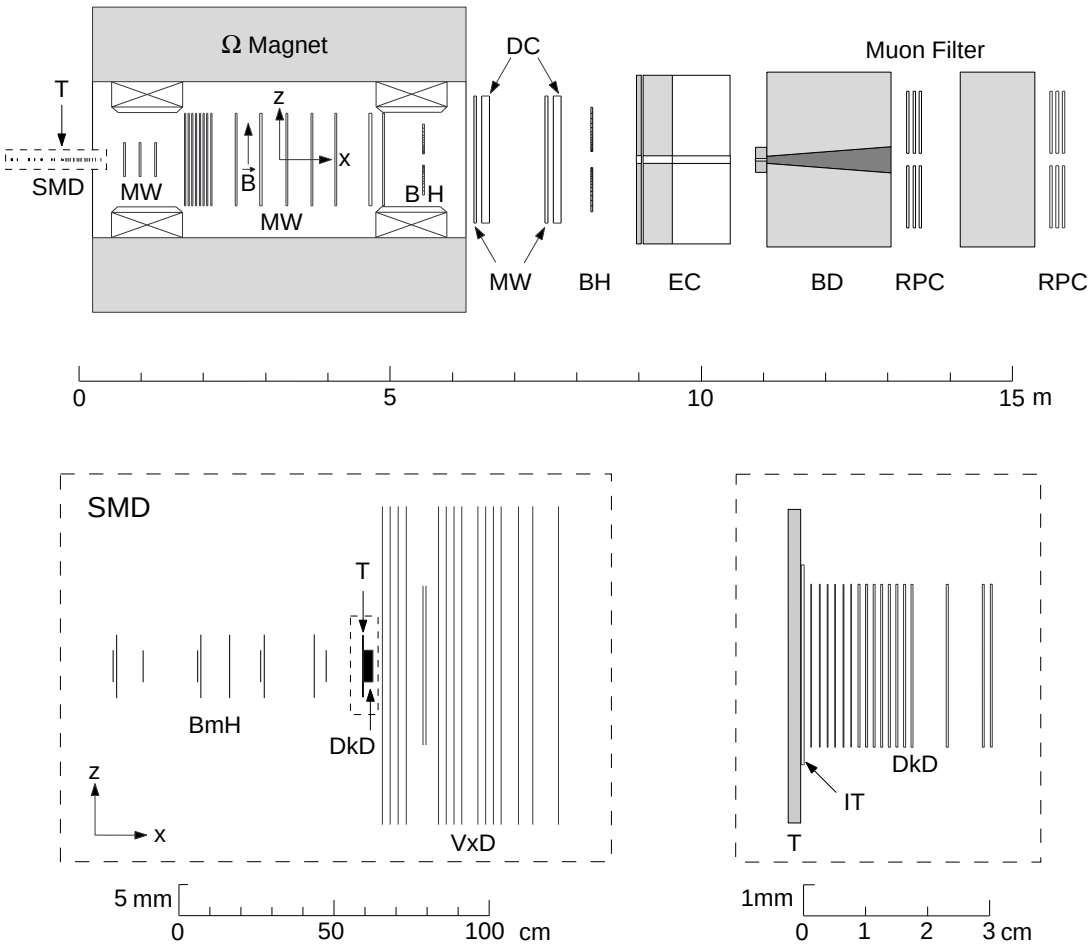

Figure 1: *Layout of the WA92 detector and the Ω Spectrometer: Target (T), silicon microstrip detectors (SMD), multiwire proportional chambers (MW), drift chambers (DC), butterfly-shaped hodoscopes (BH), electromagnetic calorimeter (EC) and muon filter comprising beam dump (BD) and resistive-plate chambers (RPC). Enlarged views show the arrangement of the SMD planes as beam hodoscope (BmH), "in-target" counter (IT), decay detector (DkD) and vertex detector (VxD).*

closely spaced in the beam direction and equipped with analogue read-out. The VxD comprised 17 silicon planes of 25- or 50-μm pitch microstrips. The IT, placed immediately downstream of the target, was a 300-μm-thick silicon microstrip plane of 200-μm pitch. It provided a fast signal if a charge equivalent to at least five minimum-ionizing particles was released in any strip. The superconducting Ω dipole magnet was equipped with multiwire and drift chambers and with two butterfly-shaped hodoscopes (BH) [7], which detected charged particles having a transverse momentum $p_T > 0.6$ GeV/c. Downstream of the magnet, after the two large Ω drift chambers, an electromagnetic calorimeter (EC) was installed; it was followed by a muon hodoscope, consisting of two iron absorbers and two sets of Resistive Plate Chambers (RPC). The first iron absorber had a tungsten core which served as a beam dump. To go through the iron absorbers the muons had to have a momentum $p_\mu > 7$ GeV/c.

WA92 adopted a combination of several independent trigger components, in order to keep the acceptance of beauty events as high as possible, with acceptable dead time. A detailed description of the trigger scheme, of its levels of implementation, of the changes introduced in the Cu93 data taking to obtain a better selectivity, and a discussion of the

acceptances, can be found elsewhere [5]. Here we simply recall the main features of this two-level trigger.

The first-level trigger (INT) selected interactions in the target. It required a triple coincidence of the beam signal, identified through scintillation counters placed upstream of the target, with the inelastic-interaction signal, provided by scintillators placed downstream of the target, above and below the beam axis, and with the "in-target" signal delivered by the IT counter. About 60 % of inelastic interactions were selected by the INT trigger.

The second-level trigger was designed to reduce the number of events selected by the first-level trigger and enrich them in beauty. It accepted events satisfying at least two of the following three conditions:

1. At least one particle detected in the butterfly hodoscopes ($p_T > 0.6$ GeV/c). This request reduced the interaction rate by a factor 2.5.
2. At least one muon detected in the muon hodoscope and pointing, in the non-bending plane, to the target region, as verified by a dedicated processor. This muon trigger had an efficiency of ~ 96 % for a single muon. It provided an inclusive muon trigger ($\geq 1\mu$) and a dimuon trigger ($\geq 2\mu$). The rate of the inclusive muon trigger was 3 % of the INT rate.
3. At least one track with impact parameter larger than 100 μm with respect to the primary vertex ("secondary track"). This condition was determined by a Beauty Contiguity Processor (BCP)[8] which used a parallel architecture for track finding and primary-vertex reconstruction. For each event, information given by the beam hodoscope and the silicon vertex detector was processed to reconstruct the primary-interaction vertex and to estimate the numbers of primary and secondary tracks. Different triggering criteria could be implemented, so that different topological requirements could be applied to the events. The acceptance rate of INT events increased from 3.9 % for 3 primary and 2 secondary tracks to 14 % for 3 primary and 1 secondary tracks. In 1993 this looser condition was used in coincidence with the muon trigger, while the coincidence between a muon and a particle with $p_T > 0.6$ GeV/c was not implemented.

With this apparatus, the number of events in the Cu92 (Cu93) data set was 4.7×10^7 (5.3×10^7), corresponding to an integrated luminosity of 2.8 (5.3) nb^{-1}[5].

2.2 Off-line reconstruction and simulation

Event reconstruction was performed using the Trident program [9], with experiment-specific modifications both in the track reconstruction and in the vertex finding algorithms. A dedicated pattern recognition procedure was developed for the high-resolution measurements in the Decay Detector and in the Silicon Vertex planes. Reconstructed tracks were matched to tracks found by Trident in the multiwire chambers and in the drift chambers. Vertex finding was based on a strategy suggested by the typical multivertex topology of the beauty events. An iterative procedure was used to define vertex candidates by creating clusters of track intersections in space. Reconstructed vertices had to be accepted by a fitting algorithm that optimized the resolution of their measurement [10, 11]. In case of ambiguities in the track–vertex associations, the tracks were assigned to the vertex to which they contributed the lowest chi-squared value.

To evaluate the acceptance of the experiment we fully simulated minimum bias, $b\bar{b}$ and $c\bar{c}$ events. Minimum bias events were generated using Fluka [12] as interfaced to

	Cu92			Cu93		
Selection	events	$b\bar{b}$	$c\bar{c}$	events	$b\bar{b}$	$c\bar{c}$
In-target inelastic interact.	1.76×10^9	100 %	100 %	3.31×10^9	100 %	100 %
Trigger	47.3×10^6	31.0 %	9.7 %	53.1×10^6	26.8 %	8.5 %
Filter	13.6×10^6	28.6 %	6.8 %	–	–	–
Sel1	13.0×10^4	14.0 %	0.74 %	40.0×10^4	11.9 %	0.80 %
Sel2	4300	3.9 %	0.04 %	11800	3.3 %	0.03 %

Table 1: *Preliminary selection: raw data reduction and simulated beauty and charm event acceptances. Relative errors on acceptance are better than* 2 %.

Geant 3.21 [13]. Events containing heavy quark ($Q\bar{Q}$) pairs were generated using a combination of Pythia 5.4 [14], this providing the description of hard processes, Jetset 7.3 [15] and Fluka. Pythia, following leading-order perturbative QCD calculations, simulates the production of a $Q\bar{Q}$ pair in a collision between a π^- having a fraction ξ of the beam-pion momentum and a nucleon. Use is made of the EHLQ [16] structure functions for nucleons and of the Owens [17] structure functions for pions. For the generation of $b\bar{b}$ events ξ is assigned a fixed value of 0.97, whereas for the generation of $c\bar{c}$ events ξ is distributed as $P(\xi) \sim \xi^5(1-\xi)$ and has a mean value of 0.75, tuned to give agreement with experimental data. The Q and the $\bar{Q}$ fragmentations are performed by Jetset in accordance with the Lund [18] string model. Information relating to the particles produced in the fragmentation is saved and the fraction of the beam-pion momentum not carried away by these particles is calculated. Fluka then simulates an interaction between a π having this calculated momentum and a target nucleus. Resonances containing heavy quarks decay according to the PDG96 [3] branching fractions. A complete event consists of the $Q\bar{Q}$ fragmentation products and the Fluka interaction products. Tracking of the particles through the experimental apparatus was performed using Geant 3.21. Detector inefficiencies and random noise were included, and the trigger response was fully simulated.

An analysis of the accuracy of our model in simulating minimum bias events can be found in ref.[5], while ref.[19] contains a comparison between experimental and simulated data for events featuring charmed-meson production.

The acceptances of the trigger for experimental data and for simulated $b\bar{b}$ and $c\bar{c}$ events are reported in Table 1, where acceptances for the off-line requirements defined below are also reported.

The total number of beauty events written on tape is of the order of 55 (90) per nb of cross-section[2)] in the Cu92 (Cu93) data.

3 Search for beauty events

The procedure for extracting beauty candidates from our data sample of $\sim 10^8$ events involves several selection steps. The selection criteria are based on the distinctive topological and kinematical features of the beauty decay chain: the presence, in the DkD region, of secondary vertices, which frequently include high-p_T hadrons or muons. The selected beauty-enriched sample is submitted to close inspection in a graphical analysis. The en-

[2)] A linear A-dependence is assumed here and for the following estimates of the number of events due to beauty production.

Cu92						
Selection	events			simulated $b\bar{b}$		
	mu	*mvtx*	*npD*	*mu*	*mvtx*	*npD*
Sel2	1101	1200	2162	2.0 %	1.64 %	0.82 %
Sel3	93	510	325	0.77 %	1.51 %	0.72 %
Scanning	3	5	2	0.46 %	0.46 %	0.17 %
Cu93						
Selection	events			simulated $b\bar{b}$		
	mu	*mvtx*	*npD*	*mu*	*mvtx*	*npD*
Sel2	2195	4005	6000	1.58 %	1.65 %	0.68 %
Sel3	245	1702	901	0.61 %	1.49 %	0.70 %
Scanning	9	7	3	0.31 %	0.39 %	0.12 %

Table 2: *Final event selection: number of events and acceptances for simulated beauty events for the three selection classes described in the text ("mu" is for μ events; "mvtx" is for multivertex events; "npD" is for non-pointing D events).*

tire selection procedure takes advantage of the imaging capability of the set-up, and in particular of the DkD, which gives a high resolution picture of the first 3 cm immediately downstream of the target.

The data reduction at each analysis step, together with the acceptances calculated from simulated events, are reported in Tables 1 and 2.

3.1 Event selection

The Cu92 data are passed through a preliminary filter, which reinforces the trigger conditions (see line 3 of Table 1). Due to the better selectivity of the Cu93 trigger, we choose not to filter the Cu93 sample.

In the first selection step (Sel1) we require at least two secondary vertices in a fiducial volume, taken as the region between 0.3 cm and 6 cm from the primary vertex, or at least one vertex in the fiducial volume together with one or more muons having $p_T > 0.6$ GeV/c. Taking advantage of the analogue read-out of the DkD, events with secondary vertices close to large energy releases, usually due to hadronic interactions in the silicon planes [5], are disregarded. The effect of this first selection step is reported in line 4 of Table 1.

In the second step (Sel2), events are selected according to their physical or topological characteristics, and are divided into three classes: μ events, *multivertex* events and *non-pointing D* events.

1. The *μ events* are events containing a muon not associated with the primary vertex and at least one secondary vertex in the fiducial volume. It is required that the muon transverse momentum be > 1.2 GeV/c if there is only one secondary vertex, or > 1.0 GeV/c if two or more secondary vertices are present. This class of events, which exploits the capabilities of the RPC muon trigger, has greatest enrichment for

the dominant fraction of beauty particles that undergo a semi-muonic decay (around 20 % of beauty events have a muon coming from a B decay).

2. The *multivertex events* are events having at least three secondary vertices in the fiducial volume and satisfying a high-p_T track requirement (at least one track with $p_T > 1.5$ GeV/c, or one track with $p_T > 0.8$ GeV/c and one track with $p_T > 0.6$ GeV/c). The conditions that define this class of events have been suggested by the large decay multiplicity for beauty, which is selected by the secondary vertex trigger (BCP).

3. In the *non-pointing* D sample, we accept events with a fully-reconstructed Cabibbo-favoured D decay, where the D does not point back to the primary vertex (*i.e.* it has an impact parameter with respect to the primary vertex ≥ 30 μm)[3], and where there is at least one other secondary vertex in the fiducial volume. The choice of this last event category , which exploits the BCP trigger, is motivated by the large fraction of B-mesons decaying into a D and by the large and clean sample of fully-reconstructed D-meson decays in our data [19].

The effects of this selection are summarized in the "Sel2" lines of Tables 1 and 2. In the latter, the contributions of the three event classes are separated. Since the selection criteria are non-exclusive, a small fraction of events belongs to more than one class.

We estimate the number of $b\bar{b}$ events remaining after the second selection step to be about 7 (11) per nb of cross-section for the Cu92 (Cu93) data.

In the last selection step (Sel3), the events that survive Sel2 undergo the following class-dependent cuts.

The μ events are filtered by imposing topological and kinematic cuts, aimed at identifying a clear signature for the semi-muonic decay of a particle heavier than charmed meson. The requirements made are:

1. any accepted secondary vertex must have two or more tracks that, in the non-bending projection, have an impact parameter with respect to the primary vertex of at least 15 μm[4];
2. the event must contain at least two accepted secondary vertices, one of which should be a μ vertex, defined as an accepted secondary vertex with an identified muon among its tracks;
3. at least one accepted vertex must have a minimum mass[5] greater than 2.3 GeV/c^2, and at least one of the remaining vertices must have a minimum mass greater than 0.55 GeV/c^2. The cut on minimum mass rejects K^0 decay vertices. Charm semileptonic decays are rejected by demanding that all μ vertices reconstructed in the DkD have minimum mass greater than 2 GeV/c^2.

The *multivertex* events tend to have a greater topological complexity than the other classes, some of the events have more than one beam particle interacting in the target within the time resolution of the detector. In order to avoid overly complex events, which are difficult to analyse, we reject those events having more than 500 hits in the DkD. This

[3] Our resolution in impact parameter reconstruction of particles decaying in the DkD is 10 μm (r.m.s.).

[4] Our resolution in the single-track impact parameter in the non-bending projection is 5 μm (r.m.s.).

[5] In calculating a vertex's minimum mass, it is assumed that the vertex corresponds to the decay of a particle from the primary vertex and that the energy-momentum conservation of the decay is ensured by an unobserved zero-mass particle.

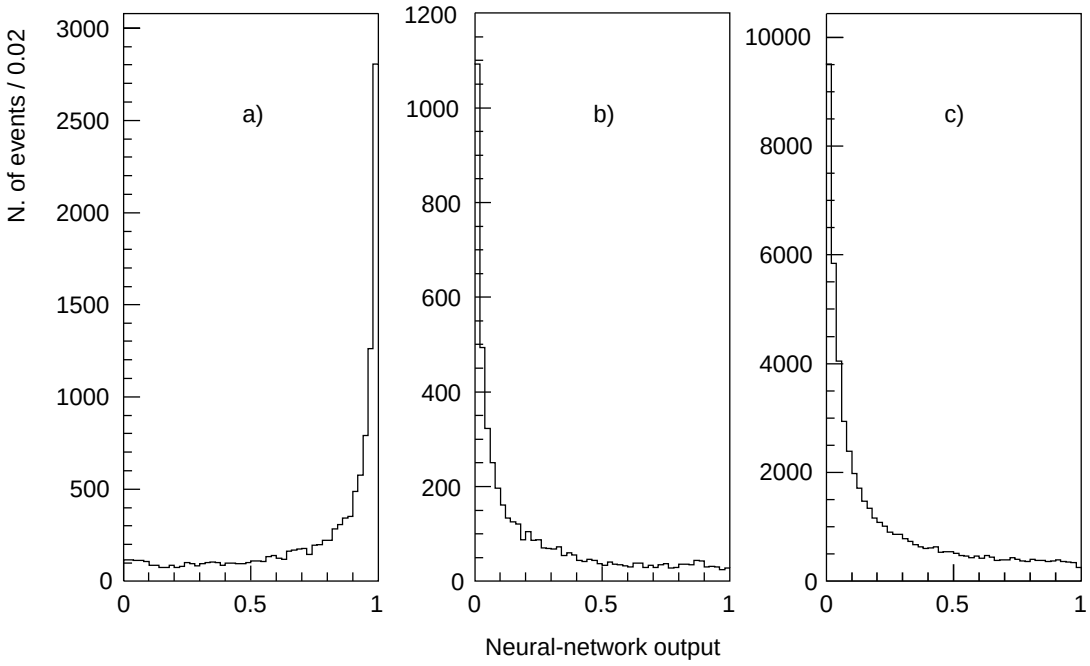

Figure 2: *Distributions of neural-network output for (a) simulated beauty events, (b) simulated charm events and (c) experimental data.*

cut does not affect simulated beauty events, but reduces by about 15 % the number of experimentally recorded events to be scanned.

The last cut in Sel3 is applied both to *multivertex* events and to *non-pointing D* events. This cut makes use of a multivariate analysis based on neural-network classifiers [20]. The neural network is trained using simulated beauty events as signal and simulated charm events and triggered data (which contain a very small fraction of beauty events) as background. Events are supplied to the neural-network through a set of 16 variables, containing both topological and kinematic information, chosen on the basis of their discriminating power between signal and background. For each event the neural-network output, which ranges from 0 to 1, is used as a tagging variable. As shown in Fig.2 the neural-network output distribution is peaked at 1 for beauty events, while, as expected, it is peaked at 0 both for simulated charm and for triggered data[6)]. We accept only the *multivertex* and *non-pointing D* events having a neural-network output > 0.6. The neural-network cut selects events on the basis of their global characteristics; stricter kinematic cuts will be applied only at the time of scanning. In Table 2, the "Sel3" line gives the effects of the class-dependent selection on the different event samples.

3.2 Event scanning

Events that survive the selection stages described above are individually analysed using a graphical display program. At the scanning level, the interpretation of events as complicated as those we have to deal with can sometimes be subjective. To avoid scanner-dependent results, we define scanning rules as rigorously as possible. Different physicists independently scan the same sample of events, and, for background and acceptance studies, the samples to be scanned contain both simulated and background events in a random

[6)] We did not use the neural-network on the μ events because the kinematical cuts described gave an equivalent enrichment factor.

order, unknown to the scanner.

The principal scanning rules are the same for the three classes of events. They require a visual quality control of tracks and vertices: primary and secondary vertices must be well reconstructed; secondary vertices in the fiducial volume must be confirmed; at least one of secondary vertices must be reconstructed in the DkD; the absence of a large energy release close to a secondary vertex must be confirmed; the secondary vertices must be well separated from one another (a $6\sigma_d$ cut on distances is applied, where our σ_d resolution in distance is of the order of 200 μm), the tracks must have the majority of their hits correctly associated and must be linked correctly to their vertex in both projections.

For the two hadronic classes we define special scanning rules.

The following criteria, optimized to discriminate between beauty events and possible background sources on the basis of kinematics, are applied to potential beauty candidates found in the *multivertex* sample:

1. none of the three vertices must be compatible with the a K^0 or a Λ^0 decay within a $3\sigma_m$ mass window, where our mass resolution σ_m is about 3 MeV/c^2 for K^0 and 1 MeV/c^2 for Λ^0;
2. at least one track linked to a candidate B decay vertex must have $p_{Tf} > 1$ GeV/c, where p_{Tf} is the transverse momentum relative to the line of flight of the decaying particle; this cut is very effective against events coming from $c\bar{c}$ decays;
3. the possible kinematic association of a beauty-charm decay chain is tested, requiring the effective mass of a reconstructed B to lie between 2.3 GeV/c^2 and 6 GeV/c^2.

Similarly, to have a clear signature for beauty events in the *non-pointing D* sample, the following criteria are applied:

1. the reconstruction of the D decay must be confirmed;
2. the D momentum must not point to the main vertex either in the non-bending projection (within 10 μm) or in the bending projection (within 20 μm), but, in both projections, its line of flight must, within errors, meet a candidate B decay vertex, which can either be another reconstructed secondary vertex or the point in which a primary track exhibits a kink;
3. if the identified D is charged (neutral), its hits must (must not) be visible on the planes crossed by its line of flight;
4. the effective mass of the B candidate chained with the reconstructed D decay must be smaller than 6 GeV/c^2.

If, during the scanning analysis, events with evident reconstruction problems are identified, we cure them by using an interactive version of Trident, in such a way as to apply the topological and kinematic cuts to correctly reconstructed events. In the interactive version of Trident the track recognition may be guided by the operator, but the track and vertex fitting algorithms are the same as in the automatic version.

The cuts applied at the scanning level result in a further acceptance reduction, and the overall beauty acceptance becomes $\approx 1\,\%$ of the triggered beauty events (see Table 2).

3.3 Beauty candidates

Beauty candidates have been identified in each of the three event classes:
12 in the μ sample,
12 in the *multivertex* sample,
5 in the *non-pointing D* sample.

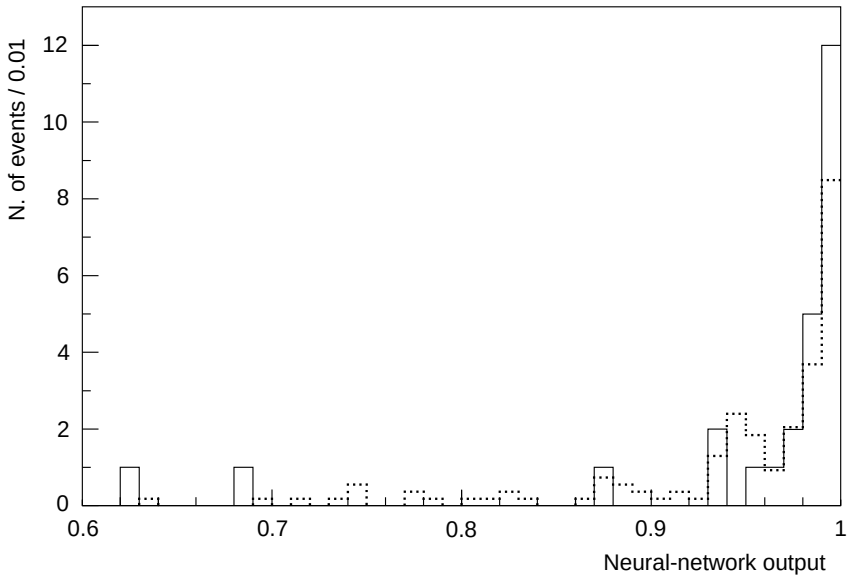

Figure 3: *Distribution of the neural-network output for events selected as beauty candidates (solid line) and for simulated $b\bar{b}$ events accepted at the scanning level and normalized in number (dotted line).*

In agreement with expectations from the simulation, one event is common to the three scanning classes and one event is common to the *multivertex* and μ classes. Our total sample then consists of 26 events.

Fig.3 shows the neural-network output for events selected as beauty candidates. The distribution is peaked at high values, indicating that the events are strong beauty candidates also in terms of the neural-network variables, and can be compared with the superimposed normalized distribution of the neural-network output for simulated $b\bar{b}$ events accepted at the scanning level.

In 15 of the 26 beauty events, the two B decay vertices are identified. The beauty candidate event common to the three classes is displayed in Fig.4. This event has three vertices in the DkD. The D vertex has a minimum mass of 1.8 GeV/c^2 relative to the more upstream B vertex, and its charge (positive) is compatible with the charge (negative) of the muon from the same B vertex. The charge of this B meson cannot be defined with much certainty, since there is only one plane between the interaction and decay vertices. However, no hit is recorded on this plane, and so our best guess is that the decay is of a $\overline{B}^0$. The associated (more downstream) B has a high p_{Tf} decay product and a large minimum mass relative to the primary vertex (4.2 GeV/c^2). The lack of hits on its line of flight from the primary vertex strongly suggests that this vertex was produced by a neutral particle, and we interpret it as B^0 decay.

3.4 Background sources

The stringent cuts applied at the analysis stage and during the scanning result in a fairly low acceptance, but were necessary to minimize the background. We identify three possible background sources for our sample of beauty candidates: charm events, nuclear interactions without nuclear breakup and events containing in-flight decay of pions and kaons into muons assigned to secondary vertices.

As the charm cross-section at our energy is 3 orders of magnitude larger than the

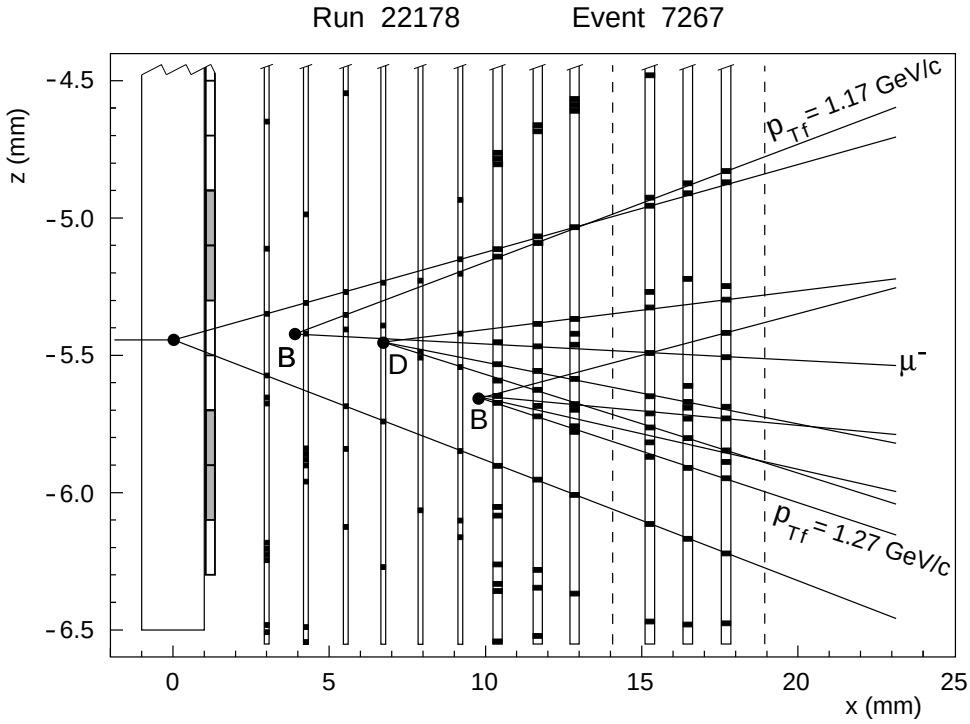

Figure 4: *Display of the beauty event which is common to the three classes described in the text. B and D decay vertices are visible. p_{Tf} indicates the transverse momentum relative to the line of flight of the parent particle.*

beauty cross-section, $c\bar{c}$ events are a potential source of background that could mimic beauty meson decays, for all three classes described above. To study this background, we simulated about two times as many $c\bar{c}$ events as were present in each of our data-taking periods. Taking into account the integrated luminosity of the experiment and the total charm hadroproduction cross-section, that we obtain from the charmed meson cross-section for $x_F > 0$ measured from our data [19] and extrapolated as suggested in [21], we estimate the production of approximately 1.7×10^6 (3.3×10^6) charm events in the Cu92 (Cu93) sample. These simulated events were processed with the same analysis and selection chain as the experimental data. The acceptances of the simulated $c\bar{c}$ events are reported in Table 1. The number of simulated $c\bar{c}$ events surviving after scanning, normalized to the number of charm events in the data, is 0 (0.6) in the Cu92 (Cu93) sample.

For beauty candidates from the *multivertex* and *non-pointing D* classes, we study possible background from white interactions, *i.e.* events in which a secondary coherent nuclear interaction occurs, without nuclear breakup and so without large energy release. We recall that secondary nuclear interactions with large energy release (black interactions) are mostly recognized and rejected using the analogue information from the DkD, and those surviving the cuts are easily identified at the scanning level.

From an analysis of minimum-bias interactions in the DkD, we estimate that the cross-section for producing white interactions is about 13 times smaller than the inelastic cross-section with nuclear breakup. Taking into account our integrated luminosities, we estimate that there are 8.7×10^6 (16.5×10^6) white interactions in the Cu92 (Cu93) data. Given these large numbers, the full simulation of a statistically significant number of white secondary nuclear interactions was impractical, because of the large CPU time needed.

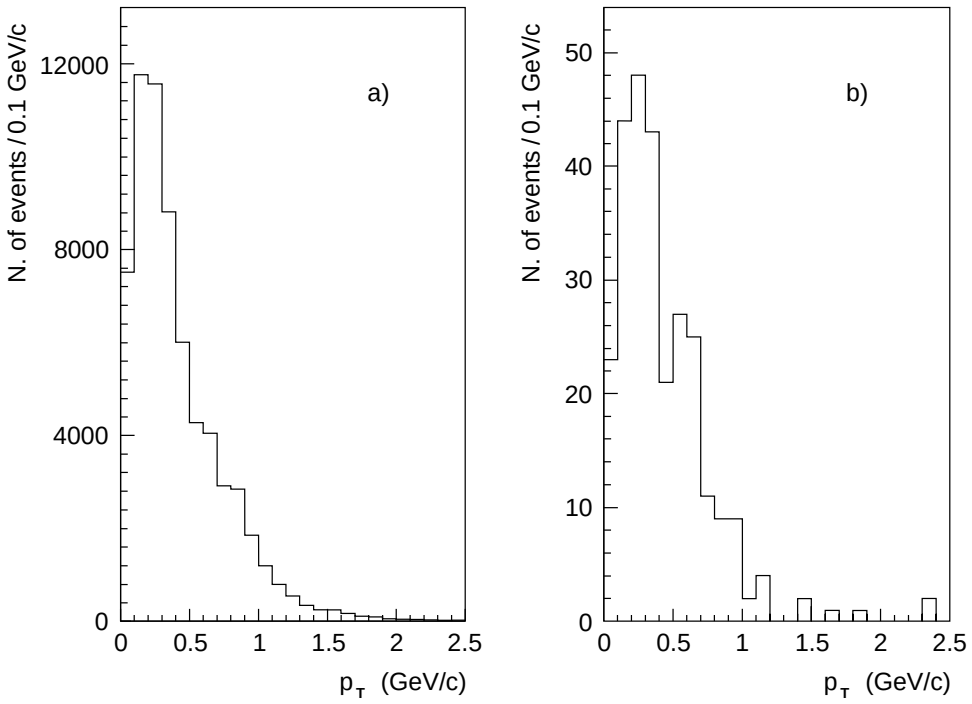

Figure 5: *Transverse momentum distribution for tracks in: "whitened" interactions (a), simulated white interactions (b).*

Instead, secondary black interactions found in the data were "whitened" by erasing the big clusters of energy release in the DkD. In Fig.5, as an example of the reliability of this method, we compare the p_T distribution of tracks from the "whitened" interactions with the same distribution for simulated white interactions. We produced a sample of "whitened" interactions corresponding to three times the estimated number of white interactions in our data. After applying the usual selection and scanning criteria, no event survives.

The beauty candidates in the muon class have been selected from events that mostly have a triggering muon produced by pion or kaon decays (a non-prompt muon). Any background event that is not a $c\bar{c}$ event will then contain a non-prompt muon. This possible contamination could in principle be studied by simulating non-prompt muon events. However the number of events to be generated would again require an unacceptable amount of CPU time. Moreover, imperfect knowledge of the kinematic features of minimum-bias events could affect the results. Our solution was to create "fake-μ" events, starting from the experimental events reconstructed by Trident. To obtain a sample of "fake-μ" events, we discard the real muon, and force the hadrons to decay into muons. As our apparatus cannot distinguish between pions and kaons, the decay kinematics is simulated assuming that the decaying hadron is a pion. These events are then weighted by the decay probability of the pion in the set-up. Since the events we are starting from have already passed the trigger selection, an additional weight, equal to the inverse of the trigger probability, is also introduced. Each initial event then generates several "fake-μ" events. These are retained if they satisfy the trigger condition and the standard selection and scanning cuts. The study of the kinematic features of these events shows that they are representative of the real background. In Fig.6, as an example, we show the minimum-mass distribution of the μ vertex for "fake-μ" events with the same distribution for triggered events.

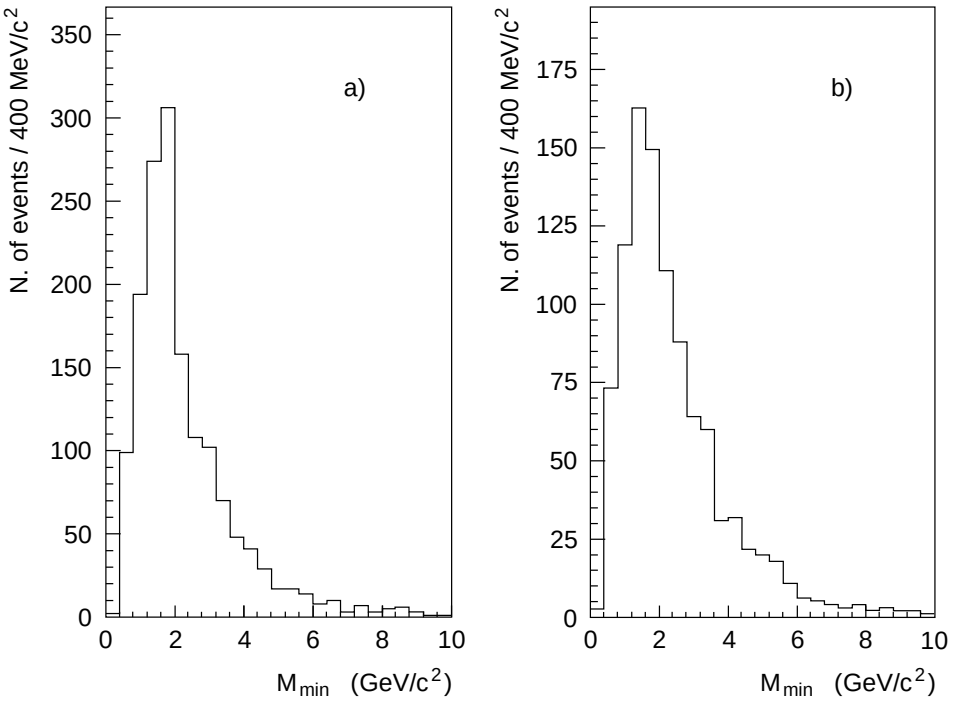

Figure 6: *Minimum mass of the μ vertex for : real data (a), and "fake-μ" events (b).*

In order to further check our procedure, and in particular the assumption that all the muons come from pions, we applied the same procedure to the large sample of simulated $c\bar{c}$ events, which contain identified pions and kaons associated to secondary vertices. We then compared, at the scanning level, the "fake-μ" generated from pions and kaons (both treated as pions) with the non-prompt muons given by Geant, and found good agreement both in numbers and kinematic features.

In order to evaluate the background to the μ events sample, we allowed for the fact that some non-prompt muons may come from $c\bar{c}$ and $b\bar{b}$ events contained in the data sample from which we started. These contributions have been evaluated from the $c\bar{c}$ and $b\bar{b}$ simulations and subtracted from the "fake-μ" event sample. The final background from non-prompt muons is zero for both the Cu92 and Cu93 data.

4 Cross-section measurement

The beauty production cross-section can be measured from each of the three selected classes: σ_μ from μ events, σ_{mvtx} from *multivertex* events and σ_{npD} from *non-pointing D* events. For a given class of events, the probability-density function (pdf) of the cross-section, $P(\sigma)$, is obtained from the convolution of the pdfs $P(\bar{N})$, $P(\bar{B})$, $P(\bar{L})$ and $P(\bar{\varepsilon})$, where $\bar{N}$, $\bar{B}$, $\bar{L}$ and $\bar{\varepsilon}$ are the "true" values of the number of beauty candidates (N), the number of background events (B), the luminosity (L) and the acceptance (ε).

The pdf $P(\bar{N})$ and $P(\bar{B})$ are inferred from the measured numbers of beauty candidates and background events, using Bayes' theorem, assuming a Poisson distribution for N and B and an *a priori* pdf that is flat in the physical region and zero outside [22]. The relative error on L is 6 %, while the relative error on ε, different for the three classes, is 9 % for the *muon* class, 12 % for the *multivertex* class, and 17 % for the *non-pointing D* class. The pdfs $P(\bar{L})$ and $P(\bar{\varepsilon})$ are assumed to be gaussians truncated at ± 3 standard deviations, these being equal to the quoted errors on L and ε. We are confident that the

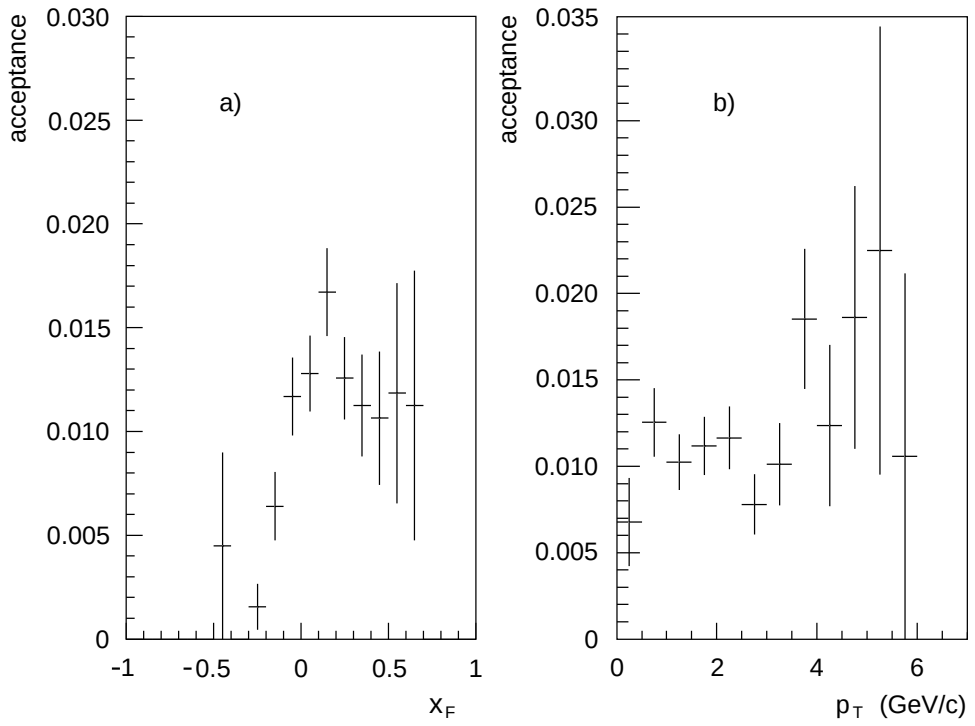

Figure 7: *Acceptance up to the visual scanning, as a function of x_F (a) and p_T (b) for simulated $b\bar{b}$ events. For each beauty event both b and $\bar{b}$ are taken considered.*

contribution to the error on ε from the assumed generation model is negligible: all the uncertainties on branching ratios and lifetimes are small [3], and the acceptance in the x_F and p_T variables is approximately constant over the region of phase space containing our events, as shown in Fig.7.

The nuclear cross-section is given by $\sigma \times A^{\alpha} = (\bar{N} - \bar{B})/(\bar{L}\bar{\varepsilon})$, where A is the nuclear mass number of the target, and α has been taken equal to 1.

If we take the best estimate of the cross-section to be the value corresponding to the maximum of $P(\sigma)$ and define the left (right) error so as to give the bounds of an interval containing a fraction 0.683 of the integral of $P(\sigma)$ below (above) its maximum, the following beauty production cross-sections, integrated over all x_F, are obtained:

for the μ class:

$$\sigma_{\mu} = 6.2^{+2.4}_{-1.7}\ (\text{stat.})^{+0.9}_{-0.6}\ (\text{syst.})\ \text{nb/N}$$

for the *multivertex* class:

$$\sigma_{mvtx} = 5.2^{+2.0}_{-1.3}\ (\text{stat.})^{+0.8}_{-0.6}\ (\text{syst.})\ \text{nb/N}$$

for the *non-pointing* D class:

$$\sigma_{npD} = 6.0^{+4.0}_{-2.5}\ (\text{stat.})^{+1.6}_{-0.8}\ (\text{syst.})\ \text{nb/N}$$

Statistical errors include the fluctuations on N and B; systematic errors take into account the uncertainties on L and ε.

The measurements relative to the three classes of events are not completely independent, but their statistical correlation is weak since only 2 of the 26 beauty candidates

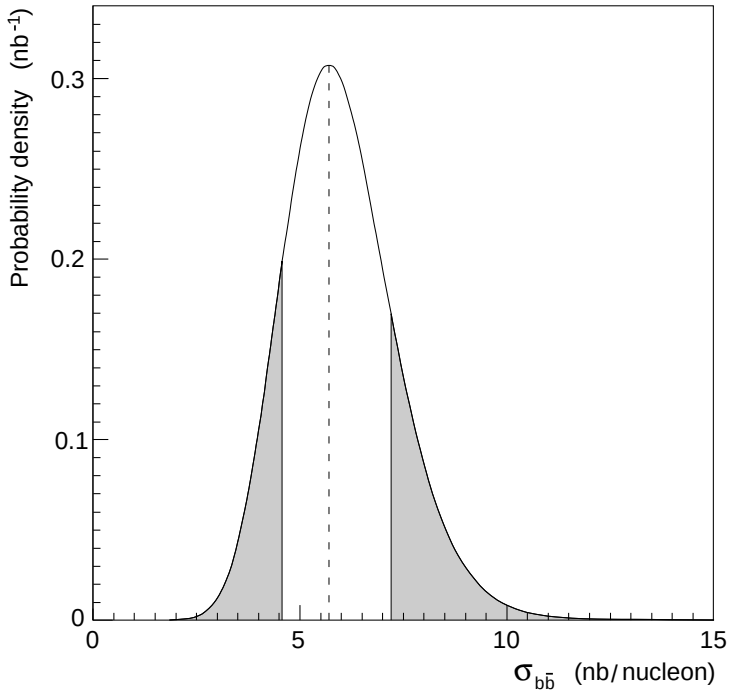

Figure 8: *Probability density function of the final beauty cross-section value. Both statistical and systematic errors contribute to the shape of this curve. The dashed line indicates the most probable value of* $\sigma_{b\bar{b}}$. *The widths of the two non-shaded bands correspond to the left and right errors, as defined in the text.*

belong to more than one category. Their agreement within errors gives us confidence in our analysis procedure.

We measure an overall cross-section using all 26 beauty candidates, independent of the class to which they belong. In this case the detection efficiency is $(0.86 \pm 0.07)\%$, slightly lower than $\varepsilon_\mu + \varepsilon_{mvtx} + \varepsilon_{npD}$ because of the partial overlap of the three classes.

Following the procedure outlined above, and again assuming a linear A-dependence, we obtain for the beauty production cross-section, integrated over all x_F:

$$\sigma_{b\bar{b}} = 5.7\ ^{+1.3}_{-1.1}\ (\text{stat.})\ ^{+0.6}_{-0.5}\ (\text{syst.}) = 5.7\ ^{+1.5}_{-1.2}\ \ \text{nb/N}$$

The errors reported in the last member of this equation are calculated by allowing all the four quantities N, B, L and ε to fluctuate according to their respective pdf. This results in the overall pdf $P(\sigma_{b\bar{b}})$ shown in Fig. 8, which provides the complete information on our cross-section measurement.

The expectation value and standard uncertainty of the $P(\sigma_{b\bar{b}})$ function are respectively 6.0 nb/N and 1.4 nb/N.

In Fig. 9 we compare the present $\sigma_{b\bar{b}}$ measurement with results obtained in previous experiments. In the low energy region our result is in good agreement with that obtained in the WA78 experiment. The high cross-section value found by the NA10 collaboration is most probably due [2] to the production mechanism assumed in their analysis, which is different from the QCD-based mechanism adopted both here and in the WA78 analysis. The theoretical predictions [1], based on a next-to-leading-order QCD calculation, are also shown in Fig. 9. They are affected by large uncertainties, depending on the values assumed for the b-quark mass and for the factorization and renormalization scales. Within

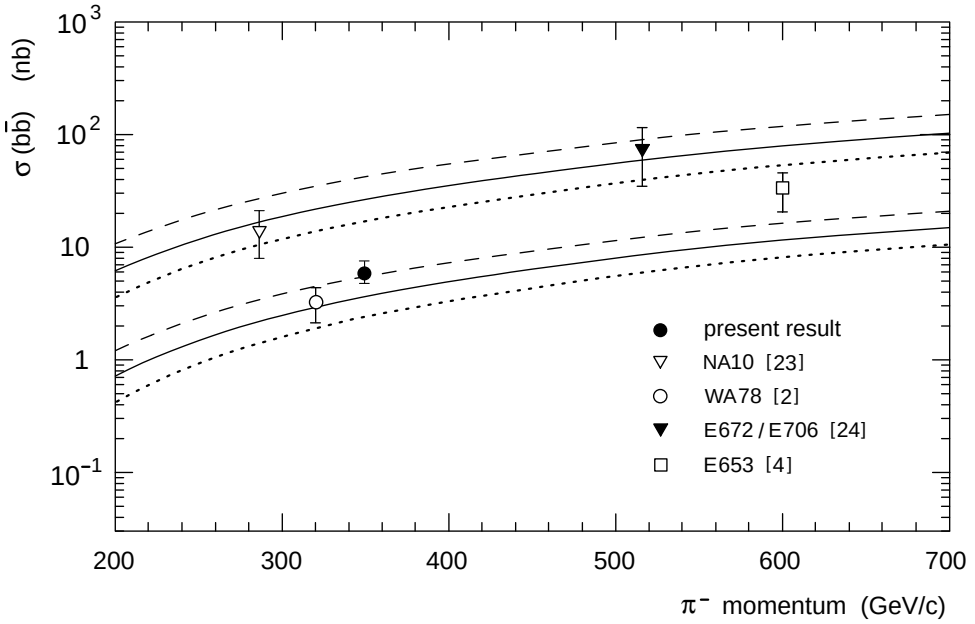

Figure 9: *Beauty cross-section measurements in $\pi^- N$ interactions compared with theoretical predictions. Theoretical uncertainty bands are obtained by varying the b-quark mass (m_b), the factorization scale (μ_F), and the renormalization scale (μ_R). Dashed band: $m_b = 4.5$ GeV/c^2; solid band: $m_b = 4.75$ GeV/c^2; dotted band: $m_b = 5$ GeV/c^2. The band widths correspond to a variation of μ_F and μ_R between $m_b/2$ and $2m_b$.*

these uncertainties, the QCD predictions are in good agreement with our result.

5 Conclusions

The WA92 experiment has recorded 26 events featuring production of beauty-particles by a 350 GeV/c π^- beam interacting in a 2-mm-thick copper target.

The beauty-particle decays are clearly identified in an imaging Decay Detector, made of high-resolution silicon microstrips, placed just downstream of the target, and their charged decay products are measured in a large acceptance spectrometer.

The background contamination is estimated to be 0.6 ± 0.6 events. Background comes mainly from secondary interactions in the material of the Decay Detector and from the production of charmed particles. The pulse height analysis for interactions occurring in the Decay Detector and the precise measurement of charm production in our experiment give us confidence in our background evaluation.

Assuming a linear A-dependence,we measure a $b\bar{b}$ cross-section, integrated over all x_F, of $5.7^{+1.3}_{-1.1}$ (stat.)$^{+0.6}_{-0.5}$ (syst.) nb/N.

6 Acknowledgements

We are grateful to G. D'Agostini and G. Ridolfi for fruitful discussions. The excellent technical support we received from the home laboratories and from the CERN Ω team was crucial for the success of this measurement.

References

[1] S. Frixione et al. Nucl. Phys. **B 431** (1994) 453.

[2] M.G. Catanesi et al., Phys. Lett. **B 231** (1989) 328.
[3] Particle Data Group, R.M. Barnett et al., Phys. Rev. **D 54** (1996) 1.
[4] K. Kodama et al., Phys. Lett. **B 303** (1993) 359.
[5] M. Adamovich et al., Nucl. Instrum. and Meth. **A 379** (1996) 252.
[6] W. Beusch et al., CERN report CERN/SPSC 77-70/T-17 (1977);
W. Beusch et al., CERN Omega group report OM/SPS/81/1 (1981).
[7] W. Beusch et al., Nucl. Instrum. and Meth. **A 249** (1986) 391.
[8] A. Beer et al.,Nucl. Instrum. and Meth. **A 337** (1994) 280.
[9] J.-C. Lassalle et al., Nucl. Instrum. and Meth. **A 176** (1980) 371.
[10] P. Billoir et al., Nucl. Instrum. and Meth. **A 241** (1985) 115.
[11] R. Fruhwirth et al., Nucl. Instrum. and Meth. **A 243** (1986) 173.
[12] A. Fassò et al., Proc. 4th International Conference on Calorimetry in High Energy Physics, La Biodola, Italy, 1993, ed. A. Menzione and A. Scribano (World Scientific, Singapore, 1994) p. 493.
[13] GEANT Detector Description and Simulation Tool, CERN Program Library Long Writeup W5013 (1994).
[14] H. U. Bengtsson and T. Sjöstrand, Comput. Phys. Commun. **46** (1987) 43.
[15] M. Bengtsson and T. Sjöstrand, Comput. Phys. Commun., **43** (1987) 367.
[16] E. Eichten et al., Rev. Mod. Phys., **56** (1984) 579;
E. Eichten et al., Rev. Mod. Phys. **58** (1985) 1065.
[17] J.F. Owens, Phys. Rev. **D 30** (1984) 943.
[18] B. Andersson et al., Phys. Rep. **97** (1983) 31.
[19] M. Adamovich et al., Nucl. Phys. **B 495** (1997) 3.
[20] L. Malferrari, Nucl. Instrum. and Meth. **A 368** (1995) 185.
[21] M. Mangano et al. Nucl. Phys. **B 405** (1993) 507.
[22] G. D'Agostini, HEP-PH/9512295, December 1995.
[23] P. Bordalo et al., Z. Phys. **C 39** (1988) 7.
[24] R. Jesik et al., Phys. Rev. Lett. **B 74** (1995) 495.